

## THE PION FORM FACTOR IN AdS/QCD

HERRY J. KWEE\* and RICHARD F. LEBED†

*Department of Physics, Arizona State University,  
Tempe, AZ 85287-1504, USA*

*\*E-mail: Herry.Kwee@asu.edu*

*†E-mail: Richard.Lebed@asu.edu  
<http://phy.asu.edu>*

Holographic QCD provides a unique framework in which to compute QCD observables. In this talk we summarize recent numerical work on computing the pion electromagnetic form factor using an AdS/QCD action that includes both spontaneous and explicit chiral symmetry breaking. We consider both hard- and soft-wall model results and develop an intermediate background that supports the best features of both. We also begin to see possible evidence in the fit for the presence of  $1/N_c$  corrections.

### 1. Introduction and Background

Studies of the duality between strongly-coupled Yang-Mills gauge theories and weakly-coupled gravity on curved backgrounds, originating with the anti-de Sitter/conformal field theory (AdS/CFT) correspondence,<sup>1</sup> have become prominent in studies of strongly-coupled field theories. In QCD, the most accessible of these theories, the approach is dubbed “AdS/QCD.” In contrast to the exact conformality of the original AdS/CFT example  $\mathcal{N}=4$  SUSY, the approximate conformality of QCD is broken by explicit mass scales such as  $\Lambda_{\text{QCD}}$  and quark masses (as evidenced by confinement and chiral symmetry breaking), which must in some manner be incorporated into the theory if one hopes to achieve a satisfactory picture for the rich spectrum and dynamics of QCD.

Since a great deal of AdS/QCD phenomenology has already been studied, even in just the meson sector,<sup>2–28</sup> we provide only a summary of the most salient features of the approach, leading eventually to a discussion of our work on the pion electromagnetic form factor  $F_\pi(Q^2)$ .<sup>27,28</sup> In the holo-

graphic approach one begins with the 5-dimensional AdS “sliced” metric,

$$ds^2 = g_{MN} dx^M dx^N = \frac{1}{z^2} (\eta_{\mu\nu} dx^\mu dx^\nu - dz^2), \quad (1)$$

where  $\eta_{\mu\nu} = \text{diag}(+, -, -, -)$  is distinguished from the full nontrivial 5D metric  $g_{MN}$  obtained from Eq. (1). One conjectures that weakly-coupled gravity on this background corresponds to strongly-coupled QCD. Crudely speaking, the  $z$  “bulk” coordinate corresponds to an inverse momentum scale:  $z \equiv \epsilon \rightarrow 0$  corresponds to the UV limit, while  $z > 0$  probes the IR behavior of the theory. Every QCD operator  $\mathcal{O}(x)$  is sourced by a 5D operator  $\Psi(x, z)$  that is uniquely determined by its boundary value  $\Psi(x, \epsilon)$ , hence the term “holographic.” The behavior of  $\Psi(x, z)$  for  $z > 0$  then encapsulates the IR dynamics. Lastly, the global symmetry of isospin is promoted to a gauged symmetry in the bulk.

## 2. Formalism

The application of these assertions provides a holographic dictionary between QCD and the 5D theory. In particular, to the QCD quark bilinear operators  $\bar{q}_L \gamma^\mu t^a q_L$ ,  $\bar{q}_R \gamma^\mu t^a q_R$ , and  $\bar{q}_R^a q_L$ , one associates the gauge fields  $A_{L\mu}^a$  and  $A_{R\mu}^a$  (with coupling  $g_5$ ), and the bifundamental field  $(2/z)X^{\alpha\beta}$ , respectively. From these one defines polar- and axial-vector fields  $V^M, A^M \equiv \frac{1}{2}(A_L^M \pm A_R^M)$ , from which one defines field strengths  $F_V^{MN} \equiv \partial^M V^N - \partial^N V^M - i([V^M, V^N] + [A^M, A^N])$  and  $F_A^{MN} \equiv \partial^M A^N - \partial^N A^M - i([V^M, A^N] + [A^M, V^N])$  and the covariant derivative  $D^M X \equiv \partial^M X - i[V^M, X] - i\{A^M, X\}$ . One further decomposes  $X = X_0 \exp(2i\pi^a t^a)$ , where the modulus field  $X_0 = \frac{1}{2}v(z)$  carries information on the form of chiral symmetry breaking (as discussed below), and the exponent is the usual nonlinear representation of pseudoscalar pion fields (in this notation, we take  $\pi \equiv \tilde{\pi}/f_\pi$ , where  $\tilde{\pi}$  is the canonically-normalized pion field and  $f_\pi = 92.1$  MeV). The lowest-order 5D action then reads

$$S = \int d^5x e^{-\Phi(z)} \sqrt{g} \text{Tr} \left\{ |DX|^2 + 3|X|^2 - \frac{1}{2g_5^2} (F_V^2 + F_A^2) \right\}, \quad (2)$$

where  $e^{-\Phi(z)}$  represents a background dilaton coupling. Working in the axial-like gauges  $V_z = A_z = 0$ , resolving  $A_\mu = A_{\mu\perp} + \partial_\mu \varphi$  into transverse and longitudinal parts, and working in momentum space, one obtains the Euler-Lagrange equations:

$$\partial_z \left( \frac{e^{-\Phi(z)}}{z} \partial_z V_\mu^a \right) + \frac{q^2 e^{-\Phi(z)}}{z} V_\mu^a = 0, \quad (3)$$

$$\left[ \partial_z \left( \frac{e^{-\Phi(z)}}{z} \partial_z A_\mu^a \right) + \frac{q^2 e^{-\Phi(z)}}{z} A_\mu^a - \frac{g_5^2 v(z)^2 e^{-\Phi(z)}}{z^3} A_\mu^a \right]_\perp = 0, \quad (4)$$

$$\partial_z \left( \frac{e^{-\Phi(z)}}{z} \partial_z \varphi^a \right) + \frac{g_5^2 v(z)^2 e^{-\Phi(z)}}{z^3} (\pi^a - \varphi^a) = 0, \quad (5)$$

$$-q^2 \partial_z \varphi^a + \frac{g_5^2 v(z)^2}{z^2} \partial_z \pi^a = 0, \quad (6)$$

$$\partial_z \left( \frac{e^{-\Phi(z)}}{z^3} \partial_z X_0 \right) + \frac{3e^{-\Phi(z)}}{z^5} X_0 = 0. \quad (7)$$

The meson masses/wave functions are then obtained as the eigenvalues/eigenfunctions of the equations of motion treated as Sturm-Liouville systems, leading to Kaluza-Klein towers of meson states reminiscent of old-fashioned Regge trajectories. Meanwhile, the source currents that create or destroy mesons appear as the free-field solutions to the equations of motion. Meson form factors are then overlap integrals (in  $z$ ) of the source solutions with the external-state eigenmode solutions. Our case of interest is the pion electromagnetic form factor  $F_\pi(Q^2)$ ; the pion wave function is the lowest-mass mode (massless in the limit  $m_q \rightarrow 0$ ) of the field  $\pi(q^2, z)$ , which is seen from Eqs. (5)–(6) to be coupled to the solution for  $\varphi(q^2, z)$ . With  $V(q, z)$  being the source current from Eq. (3) normalized by  $V(0, z) = 1$ , one obtains

$$F_\pi(q^2) = \int dz e^{-\Phi(z)} \frac{V(q, z)}{f_\pi^2} \left\{ \frac{1}{g_5^2 z} [\partial_z \varphi(z)]^2 + \frac{v(z)^2}{z^3} [\pi(z) - \varphi(z)]^2 \right\}, \quad (8)$$

which is most useful for spacelike  $Q^2$ . In the timelike region, the large- $N_c$  nature of the holographic approach gives the form factor as a sum over zero-width vector meson poles (the  $\rho$  and its excitations):

$$F_\pi(q^2) = - \sum_{n=1}^{\infty} \frac{f_n g_{n\pi\pi}}{q^2 - M_n^2}, \quad (9)$$

where  $g_{n\pi\pi}$  is given by

$$g_{n\pi\pi} = \frac{g_5}{f_\pi^2} \int dz \psi_n(z) e^{-\Phi(z)} \left\{ \frac{1}{g_5^2 z} [\partial_z \varphi(z)]^2 + \frac{v(z)^2}{z^3} [\pi(z) - \varphi(z)]^2 \right\}, \quad (10)$$

where  $\psi_n$  are the eigenmodes for the vector states. While Ref. 27 considered both  $F_\pi(Q^2)$  curves and the pattern of  $g_{n\pi\pi}$  values, in this talk we focus exclusively on the spacelike pion form factor  $F_\pi(Q^2)$  obtained from Eq. (8).

### 3. Background and Chiral Symmetry-Breaking Fields

The discussion to this point is just a straightforward application of the basic holographic scheme. To continue from this point, however, one must make two choices: for the field  $v(z)$  encapsulating the chiral symmetry breaking, and for the background field  $e^{-\Phi(z)}$ .

Addressing first the background field, we note that two popular choices permeate the literature: the hard-wall model<sup>29</sup> with step function  $e^{-\Phi(z)} = H(z_0 - z)$  and the soft-wall model<sup>2</sup> with Gaussian  $e^{-\Phi(z)} = e^{-\kappa^2 z^2}$ . We introduce<sup>28</sup> the interpolating “semi-hard” option, inspired by the Saxon-Woods model of nuclear charge density:

$$e^{-\Phi(z)} = \frac{e^{\lambda^2 z_0^2} - 1}{e^{\lambda^2 z_0^2} + e^{\lambda^2 z^2} - 2}, \quad (11)$$

which, like the hard-wall profile, has a drop-off at  $z = z_0$ , but like the soft-wall profile decreases as  $e^{-\lambda^2 z^2}$  for large  $z$ . The hard-wall model was introduced for its simplicity: The fields simply permeate a fixed distance  $z_0$  into the bulk, and the resulting meson trajectories as a function of excitation quantum number  $n$  scale as  $m_n^2 \sim n^2$ . On the other hand, semiclassical flux-tube QCD reasoning leads<sup>30</sup> to the conclusion  $m_n^2 \sim n^1$ ; the soft-wall model was developed precisely to accommodate this behavior. Unfortunately, hard-wall models tend to give more accurate predictions for QCD observables than soft-wall models; as an example,<sup>16</sup> the experimental value for the ratio  $m_\rho^2/f_\rho = 5.02 \pm 0.04$  compares favorably with the hard-wall result 5.55, but rather poorly with the soft-wall prediction 8.89 (other examples appear in Table 1). Nevertheless, as seen below, the linear trajectory of the soft-wall model is preserved simply by the exponential tail of the background, which motivates the hybrid choice in Eq. (11).

Turning now to the choice of chiral symmetry breaking represented by the field  $v(z)$ , we begin by noting that the two solutions to Eq. (7) in the hard wall case are  $z^1$  and  $z^3$ . Since the standard gauge/gravity techniques identify the operator source as the non-normalizable (more singular) solution and the state and associated vev with the normalizable (less singular) as  $z \rightarrow 0$ , one identifies<sup>3</sup> the coefficient of  $z^1$  with the quark mass and  $z^3$  with the quark condensate:  $v(z) = m_q z + \sigma z^3$ . In the soft-wall model, the exact solutions turn out to be Kummer (confluent hypergeometric) functions, which have the unfortunate feature that only one solution satisfies the appropriate boundary conditions<sup>2</sup> by vanishing asymptotically as  $z \rightarrow \infty$ . Taken literally, this unique solution would give an unphysical fixed ratio for  $m_q$  to  $\sigma$ ; as argued in Ref. 2, however, neglected higher-order terms

in the quark potential permit independent coefficients for the  $z^1$  and  $z^3$  terms in the low- $z$  expansion of the solution for  $v(z)$ . Lacking exact forms for the higher-order terms, one may implement this fact in two ways: One may note<sup>27</sup> that the soft-wall background  $e^{-\kappa^2 z^2}$  suppresses the distinction between the exact solution for  $v(z)$  and  $m_q z + \sigma z^3$  at large  $z$ , or one may choose<sup>28</sup> a modified form for  $v(z)$  that behaves like  $m_q z + \sigma z^3$  for small  $z$  and like the asymptotic form of the appropriate Kummer function for large  $z$ . In either case, one finds that the numerical solutions for static observables and  $F_\pi(Q^2)$  are never better than those of the hard-wall model.

#### 4. Numerical Solutions

This brings us to the question of how to solve Eqs. (3)–(7) in practice. In particular, Eqs. (5) and (6) are coupled, and the whole set depends upon three adjustable parameters,  $z_0$  or  $\kappa$ ,  $m_q$ , and  $\sigma$ . Analytic solutions exist only in certain limits,<sup>27</sup> particularly, as studied in Ref. 20,  $m_q \rightarrow 0$ . If  $m_q \neq 0$ , one must resort to a numerical approach, using standard techniques<sup>31</sup> such as the “shooting method” and properly convergent numerical integrations to solve the equations. Such calculations, carried out in hard, soft, and semi-hard backgrounds, form the core of our work.<sup>27,28</sup>

Figure 1 compares our  $F_\pi(Q^2)$  hard- and soft-wall model results to data. The value of  $z_0$  (hard wall) or  $\kappa$  (soft wall) is completely fixed by the value of  $m_\rho$ ; once this primary parameter is fixed, the pion decay constant  $f_\pi$  is determined by adjusting  $\sigma$ . Finally, the Gell-Mann–Oakes–Renner formula  $m_\pi^2 f_\pi^2 = 2m_q \sigma$  uses  $m_\pi$  to fix a value of  $m_q$ . Empirically, the shape of  $F_\pi(Q^2)$  is driven primarily by  $\sigma$ . Using the experimental values  $m_\rho = 775.3$  MeV,  $m_\pi = 139.6$  MeV, and  $f_\pi = 92.1$  MeV, one obtains the hard-wall parameters  $1/z_0 = 322$  MeV,  $\sigma^{1/3} = 326$  MeV, and  $m_q = 2.30$  MeV, which in turn generate the solid line in Fig. 1. The same experimental values for  $m_\rho$  and  $m_\pi$  (but taking<sup>a</sup>  $f_\pi = 87.0$  MeV) in the soft-wall model give  $\kappa = 389$  MeV,  $\sigma^{1/3} = 368$  MeV, and  $m_q = 1.45$  MeV, and produce the dashed line. Both models predict a value of  $F_\pi(Q^2)$  clearly more shallow than data, an effect even more pronounced when one views the same plot using the dependent variable  $Q^2 F_\pi(Q^2)$  [Fig. 2]. Interestingly, the discrepancy with  $F_\pi(Q^2)$  data could easily be cured if  $f_\pi$  were smaller:  $f_\pi = 64.2$  MeV ( $\sigma^{1/3} = 254$  MeV) (hard-wall) gives the dash-dot curve in Fig. 1, and  $f_\pi = 52.2$  MeV ( $\sigma^{1/3} = 262$  MeV) (soft-wall) gives the dash-dot-dot curve. We return presently to the question of the meaning of these anomalously small  $f_\pi$  values.

<sup>a</sup>The slightly smaller value used for  $f_\pi$  allows for a much improved fit to  $F_\pi(Q^2)$ .

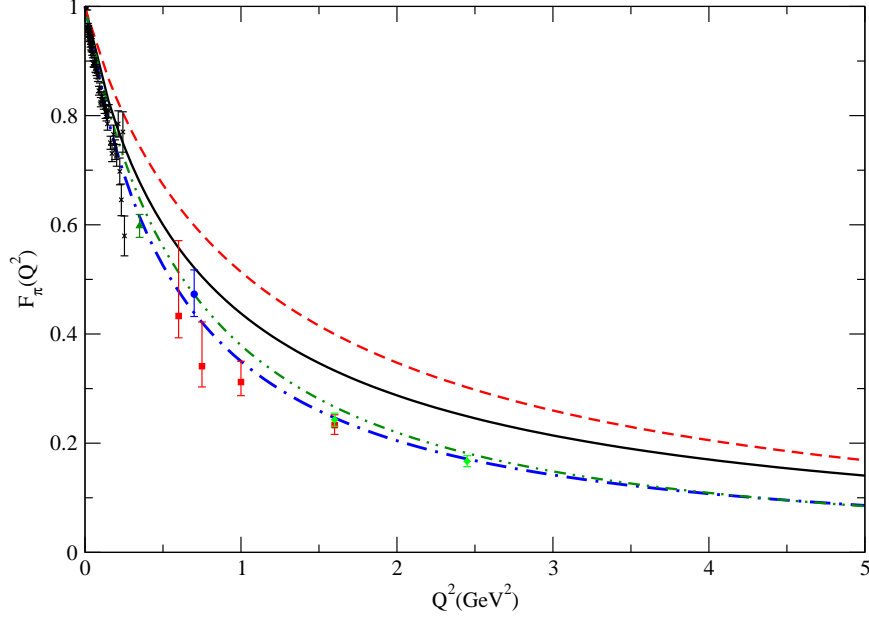


Fig. 1. The pion form factor  $F_\pi(Q^2)$  prediction in hard- and soft-wall models compared to data.<sup>32–37</sup> The solid (black online) and dash-dot (blue online) lines are hard-wall model predictions whose input parameters differ only by use of a smaller value of  $f_\pi$  than experiment in the latter, and analogously for the dashed (red online) and dash-dot-dot (green online) lines in the soft-wall model. The input values appear in the text.

Figure 2 is also interesting because it seems to suggest near-asymptotic values for  $Q^2 F_\pi(Q^2)$ . For example, if one adopts the standard abbreviation  $s_0 \equiv 8\pi^2 f_\pi^2 = 0.67 \text{ GeV}^2$ , then the original hard-wall model appears to approach at least  $Q^2 F_\pi(Q^2) \approx 1.2s_0$  as  $Q^2 \rightarrow \infty$ . In fact, the analytic  $m_q = 0$  hard-wall results of Ref. 20 for  $Q^2 F_\pi(Q^2)$ , which appear to conform closely with our numerical  $m_q \neq 0$  results, predict that  $Q^2 F_\pi(Q^2) \rightarrow s_0$  as  $Q^2 \rightarrow \infty$ , but also that  $Q^2 F_\pi(Q^2)$  overshoots its asymptote and does not return to it until values of  $Q^2 \gg 5 \text{ GeV}^2$ , at which partonic effects (absent in this holographic approach) are expected to become relevant. Note that the perturbative QCD result<sup>38</sup> for  $Q^2 F_\pi(Q^2)$  scales not as a constant, but rather falls off as  $\alpha_s(Q^2) f_\pi^2$ .

We have argued that the semi-hard background in Eq. (11), for suitable values of  $\lambda$  (or dimensionless variable  $\lambda z_0$ ), can be made to simulate either hard-wall or soft-wall backgrounds. This effect is illustrated in Fig. 3, which again presents the data and original hard- (solid) and soft-wall (dashed) re-

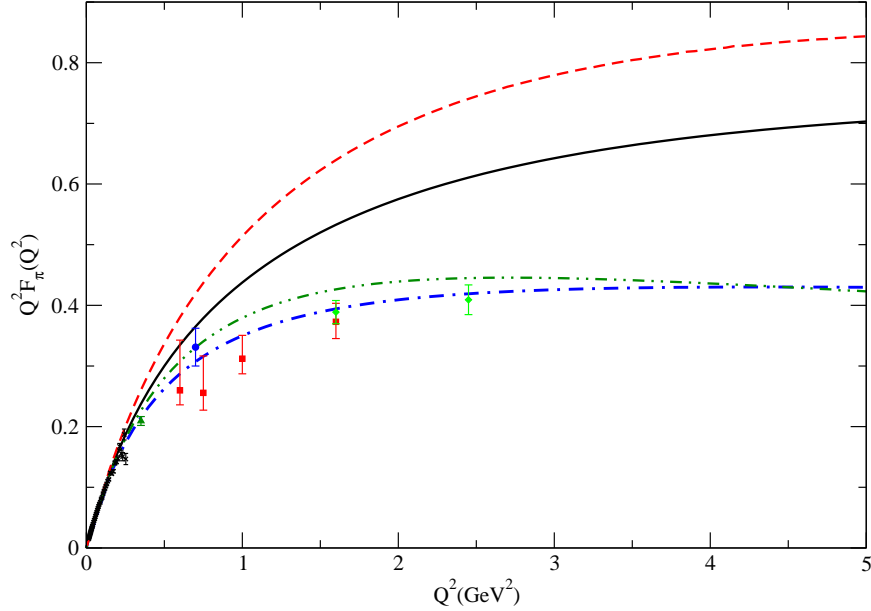


Fig. 2. The same as Fig. 1, for the combination  $Q^2 F_\pi(Q^2)$ .

sults from Fig. 1, superimposed with the result of the semi-hard model for  $\lambda z_0 = 2.1$  (crosses) and  $\lambda z_0 = 1.0$  (pluses). While the agreement between the semi-hard wall and original hard- and soft-wall models for  $F_\pi(Q^2)$  is impressive, one must check that the meson static observables (masses, decay constants, *etc.*) also agree; this is confirmed by a glance at Table 1. Despite agreeing so well with so many hard-wall quantities, the semi-hard wall model with  $\lambda z_0 = 2.1$  nevertheless generates a very different meson trajectory, as illustrated in Table 2: One finds that the exponential tail is sufficient, even for the modest value  $\lambda z_0 = 2.1$ , to turn the hard-wall  $m_n^2 \sim n^2$  trajectory into one that is  $\sim n^1$ , as a careful examination of the numbers confirms. Thus, the semi-hard wall model carries all the best features of both hard- and soft-wall models.

One mystery remains, namely, why all the models considered here using only experimental inputs predict curves for  $F_\pi(Q^2)$  too shallow compared to data (predicting, *e.g.*, too small a pion charge radius  $\langle r_\pi^2 \rangle$ ). As mentioned above, partonic degrees of freedom have not entered into the holographic calculation in any essential way; indeed, the only place that the fundamental QCD gauge theory appears is through matching<sup>3</sup> the vector-current

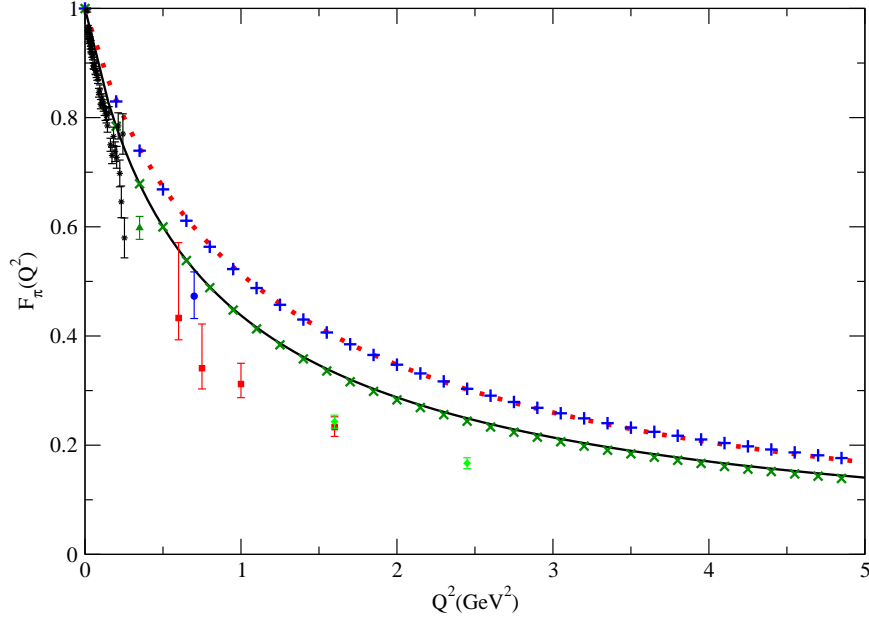


Fig. 3. Data and hard- and soft-wall model results for  $F_\pi(Q^2)$  (same symbols as in Fig. 1), superimposed with semi-hard model with  $\lambda z_0 = 2.1$  (crosses, green online) and  $\lambda z_0 = 1.0$  (pluses, blue online).

Table 1. Observables in soft- and hard-wall models compared to those from the semi-hard model of Eq. (11) with  $\lambda z_0 = 1$  and  $\lambda z_0 = 2.1$ , respectively; values in MeV (except for  $g_{\rho\pi\pi}$ , which is dimensionless).

Observable	Experiment	Soft-wall	$\lambda z_0 = 1$	Hard-wall	$\lambda z_0 = 2.1$
$m_\pi$	$139.6 \pm 0.0004^{39}$	139.6	139.6	139.6	139.6
$m_\rho$	$775.5 \pm 0.4^{39}$	777.4	779.2	775.3	777.5
$m_{a_1}$	$1230 \pm 40^{39}$	1601	1596	1358	1343
$f_\pi$	$92.4 \pm 0.35^{39}$	87.0	92.0	92.1	88.0
$f_\rho^{1/2}$	$346.2 \pm 1.4^{40}$	261	283	329	325
$f_{a_1}^{1/2}$	$433 \pm 13^{41,42}$	558	576	463	474
$g_{\rho\pi\pi}$	$6.03 \pm 0.07^{39}$	3.33	3.49	4.48	4.63

two-point function calculated both in the 5D theory and in (perturbative) QCD, from which one determines the 5D gauge coupling  $g_5 = 2\pi$ . It is natural to suppose that the holographic model is at best incomplete, due to the absence of partonic degrees of freedom; however, the accurate  $F_\pi(Q^2)$



Table 2. Comparison of vector meson masses (in MeV) from the hard-wall model and the semi-hard wall model using  $e^{-\Phi(z)}$  of Eq. (11) with  $\lambda z_0 = 2.1$ .

	$n=1$	$n=2$	$n=3$	$n=4$	$n=5$
Hard wall	775.6	1780.2	2790.8	3802.8	4815.2
Semi-hard wall	777.5	1608.1	2226.8	2637.5	2986.6

data<sup>b</sup> extends only out to  $\sim 3 \text{ GeV}^2$ , far below the regime where one would expect the partonic expression for  $F_\pi(Q^2)$  to dominate. Alternately, one might argue that the treatment of chiral symmetry used here is inadequate; while this is certainly possible, it appears to be the most realistic treatment available. These were the possible explanations proffered in Ref. 28.

However, we present here one further possible explanation: The holographic method implicitly assumes both large  $N_c$  and large 't Hooft coupling  $g_s^2 N_c$ . Can the shallow slope of  $F_\pi(Q^2)$  be a  $1/N_c$  correction?<sup>c</sup> To test this idea, we ask which quantities in the analysis are most sensitive to  $1/N_c$  corrections. While meson masses  $m_\pi$  and  $m_\rho$  are  $O(N_c^0)$ , their decay constants are  $O(N_c^{1/2})$  and thus are fractionally more sensitive to variations in  $N_c$ . Recall that the original hard-wall model gave a perfect account of the  $F_\pi(Q^2)$  data if  $f_\pi$  had been 64.2 MeV. This number is, interestingly, very close to a factor  $1-1/N_c$  smaller than the experimental value 92.1 MeV, so that their difference is easily attributable as a  $1/N_c$  correction.

While such an explanation may seem a bit glib, a similar effect has been seen long ago in the literature: The pioneering soliton model work of Adkins, Nappi, and Witten.<sup>43</sup> Using our normalization for  $f_\pi$ , their model values inserted into the Goldberger–Treiman relation  $f_\pi = M_N g_A / g_{\pi\pi N}$  predict<sup>d</sup>  $f_\pi = 61 \text{ MeV}$ , a result traditionally attributed to being due to a  $1/N_c$  correction.

These considerations suggest a supposedly “perfect” holographic model for low-energy hadronic phenomena that should include two features: A semi-hard wall background with an exponential tail extending to large  $z$ , and  $1/N_c$  corrections of a natural size, particularly for  $f_\pi$ . The semi-hard wall model has been seen to give a fit to low-energy observables just as good as that of the hard-wall model, but nevertheless generates the desired linear trajectories for excited mesons. Meanwhile, allowing  $f_\pi$  to be smaller

<sup>b</sup>Some  $F_\pi(Q^2)$  data points extend out to about  $10 \text{ GeV}^2$ , but the uncertainties are sufficiently large as to accommodate almost any model.

<sup>c</sup>That the discrepancy can be a  $1/g_s^2 N_c$  correction was suggested to us by O. Andreev.

<sup>d</sup>Reference 43 actually used the Goldberger–Treiman relation to predict  $g_{\pi\pi N}$ .

by a relative  $1/N_c$  correction is sufficient to correct the shallowness of the  $F_\pi(Q^2)$  curves compared to experiment. Indeed, it is remarkable that these modifications are sufficient to cure the discrepancies with data but still make no mention of the partonic degrees of freedom in QCD. A truly perfect holographic model would of necessity incorporate dynamical quarks as well.

## 5. Conclusions

Since their inception, holographic methods have provided a compelling theoretical framework in which to study hadronic quantities, including  $F_\pi(Q^2)$ . In this talk we have seen that the choice of background field behavior has a strong effect on low-energy observables, but it is possible to retain many of the best features of each model while adjusting this background; the semi-hard wall background proves ideal for accomplishing this goal. In passing, we note that the treatment of chiral symmetry breaking advocated by Ref. 3 appears completely suitable for this purpose. However, we begin to see in the precise value of the slope of  $F_\pi(Q^2)$  possible evidence for the necessity of including  $1/N_c$  corrections in order to achieve completely satisfactory agreement with data. The great remaining challenge appears to be how to knit together the promising first results of this all-hadronic approach with the fundamental QCD partonic degrees of freedom.

## Acknowledgments

RFL thanks the organizers for their kind invitation and an interesting scientific program. This presentation benefited from discussions with H. Grigoryan and A. Radyushkin. This work was supported by the NSF under Grant No. PHY-0456520.

## References

1. J.M. Maldacena, Adv. Theor. Math. Phys. **2**, 231 (1998) [Int. J. Theor. Phys. **38**, 1113 (1999)] [arXiv:hep-th/9711200]; S.S. Gubser, I.R. Klebanov, and A.M. Polyakov, Phys. Lett. B **428**, 105 (1998) [arXiv:hep-th/9802109]; E. Witten, Adv. Theor. Math. Phys. **2**, 253 (1998) [arXiv:hep-th/9802150].
2. A. Karch, E. Katz, D.T. Son, and M.A. Stephanov, Phys. Rev. D **74**, 015005 (2006) [arXiv:hep-ph/0602229].
3. J. Erlich, E. Katz, D.T. Son, and M.A. Stephanov, Phys. Rev. Lett. **95**, 261602 (2005) [arXiv:hep-ph/0501128].
4. H. Boschi-Filho and N.R.F. Braga, JHEP **0305**, 009 (2003) [arXiv:hep-th/0212207].
5. G.F. de Teramond and S.J. Brodsky, Phys. Rev. Lett. **94**, 201601 (2005) [arXiv:hep-th/0501022].

6. N. Evans and A. Tedder, Phys. Lett. B **642**, 546 (2006) [arXiv:hep-ph/0609112].
7. P. Colangelo, F. De Fazio, F. Jugeau and S. Nicotri, Phys. Lett. B **652**, 73 (2007) [arXiv:hep-ph/0703316].
8. H. Forkel, M. Beyer and T. Frederico, JHEP **0707**, 077 (2007) [arXiv:0705.1857 (hep-ph)].
9. L. Da Rold and A. Pomarol, Nucl. Phys. B **721**, 79 (2005) [arXiv:hep-ph/0501218]; JHEP **0601**, 157 (2006) [arXiv:hep-ph/0510268].
10. J. Hirn and V. Sanz, JHEP **0512**, 030 (2005) [arXiv:hep-ph/0507049]; J. Hirn, N. Rius and V. Sanz, Phys. Rev. D **73**, 085005 (2006) [arXiv:hep-ph/0512240].
11. K. Ghoroku, N. Maru, M. Tachibana and M. Yahiro, Phys. Lett. B **633**, 602 (2006) [arXiv:hep-ph/0510334].
12. T. Huang and F. Zuo, arXiv:0708.0936 [hep-ph].
13. H. Boschi-Filho, N.R.F. Braga and C.N. Ferreira, Phys. Rev. D **73**, 106006 (2006) [Erratum-ibid. D **74**, 089903 (2006)] [arXiv:hep-th/0512295]; O. Andreev and V.I. Zakharov, Phys. Rev. D **74**, 025023 (2006) [arXiv:hep-ph/0604204]; C.D. White, Phys. Lett. B **652**, 79 (2007) [arXiv:hep-ph/0701157].
14. T. Hambye, B. Hassanain, J. March-Russell and M. Schvellinger, Phys. Rev. D **74**, 026003 (2006) [arXiv:hep-ph/0512089]; Phys. Rev. D **76**, 125017 (2007) [arXiv:hep-ph/0612010].
15. H.R. Grigoryan and A.V. Radyushkin, Phys. Lett. B **650**, 421 (2007) [arXiv:hep-ph/0703069].
16. H.R. Grigoryan and A.V. Radyushkin, Phys. Rev. D **76**, 095007 (2007) [arXiv:0706.1543 (hep-ph)].
17. S. Hong, S. Yoon and M.J. Strassler, JHEP **0604**, 003 (2006) [arXiv:hep-th/0409118].
18. A.V. Radyushkin, Phys. Lett. B **642**, 459 (2006) [arXiv:hep-ph/0605116].
19. S.J. Brodsky and G.F. de Téramond, Phys. Rev. D **77**, 056007 (2008) [arXiv:0707.3859 [hep-ph]].
20. H.R. Grigoryan and A.V. Radyushkin, Phys. Rev. D **76**, 115007 (2007) [arXiv:0709.0500 [hep-ph]].
21. H. R. Grigoryan and A. V. Radyushkin, Phys. Rev. D **77**, 115024 (2008) [arXiv:0803.1143 [hep-ph]].
22. P. Colangelo, F. De Fazio, F. Giannuzzi, F. Jugeau and S. Nicotri, arXiv:0807.1054 [hep-ph].
23. W. de Paula, T. Frederico, H. Forkel and M. Beyer, arXiv:0806.3830 [hep-ph].
24. S.S. Agaev and M.A.G. Nobary, Phys. Rev. D **77**, 074014 (2008) [arXiv:0805.0993 [hep-ph]].
25. D. f. Zeng, arXiv:0805.2733 [hep-th].
26. B. Batell and T. Gherghetta, Phys. Rev. D **78**, 026002 (2008) [arXiv:0801.4383 [hep-ph]].
27. H.J. Kwee and R.F. Lebed, JHEP **0801**, 027 (2008) (arXiv:0708.4054 [hep-ph]).
28. H. J. Kwee and R. F. Lebed, Phys. Rev. D **77**, 115007 (2008) [arXiv:0712.1811]

- [hep-ph]].
29. J. Polchinski and M.J. Strassler, Phys. Rev. Lett. **88**, 031601 (2002) [arXiv:hep-th/0109174].
  30. M. Shifman, arXiv:hep-ph/0507246.
  31. William H. Press, Brian P. Flannery, Saul A. Teukolsky, William T. Vetterling, *Numerical Recipes in FORTRAN 77: The Art of Scientific Computing*, (Cambridge University Press, 1992).
  32. S.R. Amendolia *et al.*, Phys. Lett. B **138**, 454 (1984); Nucl. Phys. **B277**, 168 (1986).
  33. P. Brauel *et al.*, Phys. Lett. B **69**, 253 (1977); P. Brauel *et al.*, Z. Phys. C **3**, 101 (1979).
  34. V. Tadevosyan *et al.* [Jefferson Lab F(pi) Collaboration], Phys. Rev. C **75**, 055205 (2007) [arXiv:nucl-ex/0607007].
  35. H. Ackermann *et al.*, Nucl. Phys. **B137**, 294 (1978).
  36. T. Horn *et al.* [Fpi2 Collaboration], Phys. Rev. Lett. **97**, 192001 (2006) [arXiv:nucl-ex/0607005].
  37. C.J. Bebek *et al.*, Phys. Rev. D **17**, 1693 (1978).
  38. G.P. Lepage and S.J. Brodsky, Phys. Lett. B **87**, 359 (1979); A.V. Efremov and A.V. Radyushkin, Theor. Math. Phys. **42**, 97 (1980) [Teor. Mat. Fiz. **42**, 147 (1980)].
  39. S. Eidelman *et al.* (PDG), Phys. Lett. B **592**, 1 (2004).
  40. J.F. Donoghue, E. Golowich, and B.R. Holstein, *Dynamics of the Standard Model* (Cambridge University Press, Cambridge 1992)
  41. N. Isgur, C. Morningstar, and C. Reader, Phys. Rev. D **39**, 1357 (1989).
  42. D.T. Son and M.A. Stephanov, Phys. Rev. D **69**, 065020 (2004) [arXiv:hep-ph/0304182].
  43. G.S. Adkins, C.R. Nappi and E. Witten, Nucl. Phys. B **228**, 552 (1983).